

## Wet Adhesive Properties of Asian Green Mussel (*Perna viridis*) Foot Protein Pvfp-5: An Underwater Adhesive Primer

### *Propiedades Adhesivas Húmedas de la Proteína del Pie de Mejillones Verdes Asiático (*Perna viridis*) Pvfp-5: Una Base Adhesiva Subacuática*

Navinkumar J Patil<sup>1</sup>\*, Paola Gabriela Vinueza Naranjo<sup>2</sup>, Bruno Zappone<sup>3</sup>

<sup>1</sup>Dipartimento di Fisica, Università della Calabria, Arcavacata di Rende (CS), 87036, Italy.

<sup>2</sup>DIET, Sapienza Università di Roma, Roma (RM), Italy.

<sup>3</sup>Consiglio Nazionale delle Ricerche, Istituto di Nanotecnologia (CNR-Nanotec), Rende (CS) 87036, Italy;  
[paola.vinueza@uniroma1.it](mailto:paola.vinueza@uniroma1.it); [bruno.zappone@cnr.it](mailto:bruno.zappone@cnr.it)

\* Correspondence: [navinjpatil@gmail.com](mailto:navinjpatil@gmail.com)

Recibido 30 octubre 2018; Aceptado 28 noviembre 2018; Publicado 10 diciembre 2018

**Abstract:** Asian green mussels (*Perna viridis*) are bivalves that attach firmly to rocks in wave-battered intertidal seashores via a proteinaceous secretion. *P. viridis* mussels follow a precisely time-regulated secretion of adhesive proteins where *P. viridis* foot protein-5 (Pvfp-5) was identified as the first protein to be secreted during the formation of adhesive plaque. The high content of catecholic amino acid 3,4-dihydroxy-L-phenylalanine (DOPA) (~11 mol%) and cysteine (Cys) (~15 mol%) in Pvfp-5 and its localization near the plaque-substrate interface have prompted speculation that the vanguard protein Pvfp-5 plays a key role as an adhesive primer in underwater adhesion of *P. viridis* mussels. Surface Force Apparatus (SFA) was used to probe the adhesive properties of Pvfp-5 at the nano-scale where pH dependent wet adhesion and antioxidant activity of foot-extracted and purified Pvfp-5 were investigated. The study revealed that Pvfp-5 with its high DOPA and CYS-content maintains adhesion even at higher pH by overcoming the spontaneous oxidation of DOPA to quinone. SFA results are consistent with the apparent function of Pvfp-5 acting as an adhesive primer, overcoming repulsive hydration forces by displacing surface-bound water and generating strong and durable surface adhesion. Our findings reveal molecular-scale insights that should prove relevant and impact material sciences to help the development of new generation of wet-resistant adhesives, coatings and glues for biomedical, therapeutic and antifouling applications.

**Keywords:** Adhesion, Cysteine (CYS), Dihydroxy-L-phenylalanine (DOPA), Mussel foot proteins (Mfpps), *Perna viridis* foot protein (Pvfp), Surface Forces Apparatus (SFA)

**Resumen:** Los mejillones verdes asiáticos (*Perna viridis*) son bivalvos que se adhieren firmemente a las rocas en las costas intermareales golpeadas por las olas a través de una secreción proteica. Los mejillones de *P. viridis* siguen una secreción de proteínas adhesivas regulada en el tiempo, donde la proteína del pie-5 de *P. viridis* (Pvfp-5) fue identificada como la primera proteína que se secreta durante la formación de la placa adhesiva. El alto contenido de aminoácido catecólico 3,4-dihidroxi-L-fenilalanina (DOPA) (~11% en moles) y cisteína (Cys) (~15% en moles) en Pvfp-5 y su localización cerca de la interfaz placa-sustrato tienen provocado la especulación de que la proteína de vanguardia Pvfp-5 desempeña un papel clave como imprimación adhesiva en la adhesión bajo el agua de los mejillones de *P. viridis*. El aparato de fuerza de superficie (SFA) se usó para probar las propiedades adhesivas de Pvfp-5 a escala nanométrica, donde se investigó la adhesión húmeda dependiente del pH y la actividad antioxidante de Pvfp-5 purificado y extraído con el pie. El estudio reveló que Pvfp-5 con su alto contenido de DOPA y CYS mantiene la adhesión incluso a un pH más alto al superar la oxidación espontánea de DOPA a quinona. Los resultados de SFA son consistentes con la función aparente de que Pvfp-5 actúa como imprimación adhesiva, superando las fuerzas de hidratación repulsivas al desplazar el agua unida a la superficie y generando una adhesión superficial fuerte y duradera. Nuestros hallazgos revelan conocimientos a escala molecular que deberían ser relevantes e impactar en las ciencias de los materiales para ayudar al desarrollo de la nueva generación de adhesivos, recubrimientos y pegamentos resistentes a la humedad para aplicaciones biomédicas, terapéuticas y antiincrustantes.

**Palabras clave:** Adhesión, Cisteína (CYS), Dihidroxi-L-fenilalanina (DOPA), Proteínas del pie de mejillón (Mfpps), *Perna viridis* proteína del pie (Pvfp), Aparato de fuerzas de superficie (SFA).



# 1 Introduction

Animal attachment to a substrate is very different in terrestrial and aquatic environments. In terrestrial environment, gravity is considered as the most important detachment force. However, in submerged conditions gravity is nearly balanced out by buoyancy but flow forces such as drag and lift are of higher importance (Ditsche *et al.* 2014). As is well known, water or moisture significantly compromises the performance of most man-made adhesives, as water effectively competes for surface bonding and eliminates contributions of van der Waals interactions (Comyn, 1981; Lee *et al.* 2011).

Despite these prevalent challenges and the harshness of the physical environment, wave-swept rocky shores and ship hulls are home to a variety of organisms that have evolved to attach themselves permanently to variety of substrates that are wet, saline, corroded, and/or fouled by biofilms. Figure 1 shows variety of invertebrate animals attached underwater to wave-swept rocks and ship hulls that have evolved separate and distinct working strategies for their particular underwater bonding requirements to protect themselves against biological, chemical, and mechanical stresses from the ocean (Wilker, 2010; Stewart *et al.* 2011).

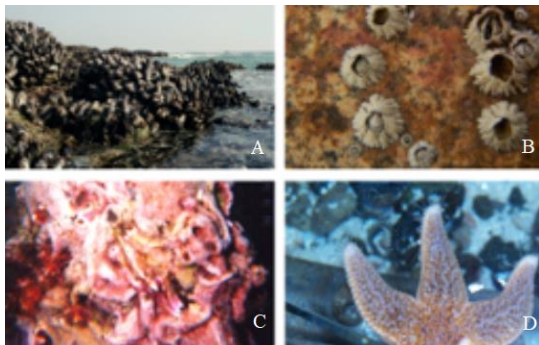


Figure 1: Mussels, barnacles, and tube worms sticking to rocks (A-C); a starfish is shown adhering to a sheet of glass (D). Figure adopted from (Wilker, 2010).

Mussels are prominent examples of sessile type organisms attaching themselves permanently to variety of underwater solid substrates. A detailed study on *Mytilus* genus (blue mussels) during the last decade has enhanced our understanding of underlying biochemical and biophysical adaptations of mussels for opportunistic and durable adhesion to moist mineral and metal oxide surfaces (Yu *et al.* 2011a; Wei *et al.* 2013; Yu *et al.* 2013). Mussel adhesion is mediated by a holdfast structure known as the byssus, essentially a bundle of macroscopic extensible high-performance fibers tipped by flattened adhesive plaques that tether the mussel firmly to a variety of hard surfaces and play a critical role in the ability of mussels to dominate space on many temperate shores

worldwide (Waite *et al.* 2005; Lin *et al.* 2007; Priemel *et al.* 2017). Byssal thread consists of several collagen-like proteins responsible for the mechanical properties of the fibers while the plaque is composed of number of protein-based adhesives containing 3,4-dihydroxyphenylalanine (DOPA), a post translationally modified amino acid that forms hydrogen bonds with almost any surface chemistry under wet conditions. Mussels adhere to surfaces underwater through the secretion, deposition, and complexation of these DOPA-containing proteins, known as mussel foot proteins (Mfps), to resist the forces produced by crashing waves – a feat unmatched by current industrial glues (Priemel *et al.* 2017; Hamada *et al.* 2017).

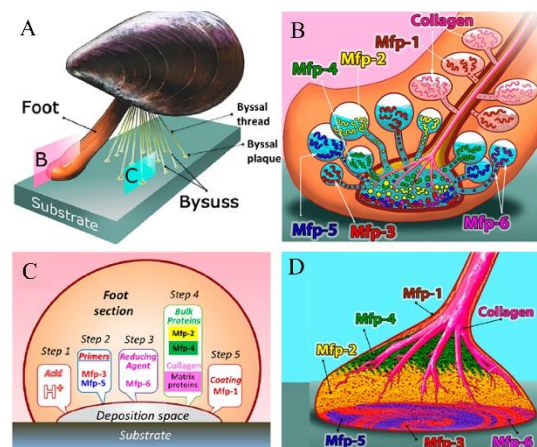


Figure 2: Cartoon of mussel byssus and proposed model of mussel's adhesion mechanism. (A) schematic overview of a mussel; (B) schematic of Mfps delivery from different precursors under mussel's foot; (C) Mfp incremental secretion: step 1, acid; step 2, primers (mfp-3 and mfp-5); step 3, reducing agent (mfp-6); step 4, bulk adhesives (mfp-2 and mfp-4) and collagen; and step 5, coating proteins (mfp-1); (D) schematic showing the distribution of major mfp's and collagen in byssal plaque. Figure adopted from (Kollbe Ahn, 2017).

Within the adhesive plaque of blue mussels (*Mytilus* species), six major mussel foot proteins (Mfp's 1-6) have been identified with substantially different amino acid sequences which are responsible for adhesion and coating of the mussel byssus (Kollbe Ahn *et al.* 2017; Lu *et al.* 2013). Each Mfp is found at a different location in the foot and byssus, and each one is believed to play a distinct and important role, as shown in figure 2 (Ahn *et al.* 2017; Silverman *et al.*, 2007; Hwang *et al.* 2010). Mfps are polyelectrolytes distinguished by their isoelectric point (pI ~ 10) and mussels appear to gain surface access for their adhesive proteins by using their own protein-based ions to outcompete the ions in their saltwater environment (Wilker, 2015). Also, the adhesive proteins found near the plaque-substrate interface are the proteins with the highest amount of DOPA, thus prompting the important and involvement of DOPA in

surface adhesion. DOPA contains a chemical group called catechol (3,4-dihydroxyphenyl), made from a benzene ring bearing two adjacent hydroxyl (-OH) groups, as shown in figure 3. Further studies on catecholic amino acid revealed that the hydroxyl groups of the catechol form chemical bonds with rocks and other substrates that help to stick the mussel in place (Ornes, 2013).

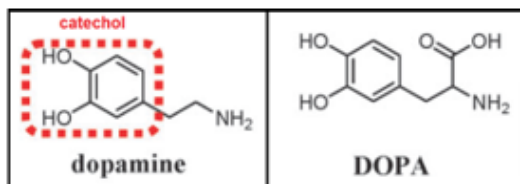


Figure 3: Dopamine and DOPA showing catechol moiety.

Although DOPA-mediated wet adhesion is strong and versatile on different surfaces, it has a troubling tendency to readily oxidize to Dopa-quinone and formation of Dopaquinone diminishes adhesion of Mfps to surfaces by at least 80-95%. There are several factors which may lead to oxidation of DOPA to Dopa-quinone. Spontaneous oxidation occurs at alkaline pH and auto-oxidation which refers to spontaneous oxidation of catechol in the presence of oxygen at neutral pH leads to loss of adhesion of Mfps (Lee *et al.* 2006; Menyo *et al.* 2013). Regulation of redox in the adhesive byssus of marine mussels is an exotic and fascinating case in point of extracellular redox where higher cysteine (CYS) content in some Mfps reduces the risk of DOPA oxidation.

Recently identified byssal plaque proteins from the Asian green mussel *Perna viridis* known as Pvfps are all enriched with cysteine (CYS) and DOPA-residues unlike Mfps, where only particular variant of plaque protein (e.g. Mfp-6) has high CYS content which acts as an anti-oxidant, reducing dopamine back to DOPA. Also, the primary sequences of Pvfps share very low homology with earlier studied Mfps (Petroni *et al.* 2015).

Our current knowledge on the nature and properties of mussel adhesion is based only on the limited set of mussel species studied. Therefore, understanding the molecular basis of adhesion in green mussels can lead us to alternate mussel inspired bioadhesives and targeted anti-fouling strategies.

Natural foot proteins from mussels of *P. viridis* were extracted by artificially inducing the live mussels to secrete plaque-forming proteins which were collected from the groove at the tip of the foot organ (Petroni *et al.* 2015; DeMartini *et al.* 2017).

It was identified that the byssal plaque proteins were secreted in time-regulated manner where *Perna viridis* foot protein-5 (Pvfp-5) was the first protein secreted by Asian green mussels to initiate interaction with the

substrate, displacing interfacial water molecules and forming adhesive bonds with the substrate which was then followed by other variants of Pvfps. Pvfp-5, which typically appeared after 10 s of saline injection, had molecular weight (MW) in the range 8-10 kDa and pI 9.2.

Amino acid sequence of Pvfp-5 revealed that it contained 12 CYS residues, accounting for 15 mol% of its amino-acid content. It also revealed 21 mol% Tyr side chains in its primary sequence and 9 DOPA residues accounting for 11 mol% DOPA in Pvfp-5. Pvfp-5 predominantly exhibited random coil structure and the dynamic light scattering (DLS) revealed a hydrodynamic diameter,  $d_H = 9.50 \pm 0.26$  nm (Petroni *et al.* 2015).

Here we report on our investigation of the attractive forces and work of adhesion between thin films of purified Pvfp-5 under changing pH conditions. The results support the conclusion that distinct mussel species adopt different strategies for underwater adhesion, where Pvfp-5 unlike Mfp-5 maintains adhesion even at higher pH due to its high DOPA and CYS content and CYS-based redox activity.

## 2 Methodology

### 2.1 Extraction and Purification of Mussel Foot Protein

*P. Viridis* foot protein (Pvfp-5) was extracted from the foot organ of *P. viridis* mussels collected from the northern coast of Singapore. Methodology for extraction and purification of Pvfp-5 has been previously reported (Petroni *et al.* 2015). The secretion of adhesive foot proteins of *P. Viridis* mussels was triggered by injecting 1 ml of KCl phosphate buffer (0.56M, pH 7.2) into the mussels pedal nerve located at the base of the foot.

Injecting KCl solution in the foot organ reasonably mimics the natural byssus secretions of *P. viridis*, and is referred as saline-induced mussel secretion. These secretions of *P. viridis* were then collected from the groove at the tip of the foot organ.

### 2.2 Surface Forces Apparatus (SFA)

Adhesion and normal force measurements between Pvfp-5 layers adsorbed on smooth and chemically inert surfaces of mica (a common alumino-silicate clay mineral) were obtained using the a SFA Mark III (Surforce LLC, Santa Barbara, CA, USA). Figure 4 shows a detailed schematic diagram of the SFA set-up used in this study. The SFA is a technique to measure the interaction forces between two macroscopic surfaces as a function of absolute distance between them using multiple beam interferometry (MBI) and

fringes of equal chromatic order (FECO). A detailed description of the technique can be found in Israelachvili & McGuigan (Israelachvili *et al.* 1990).

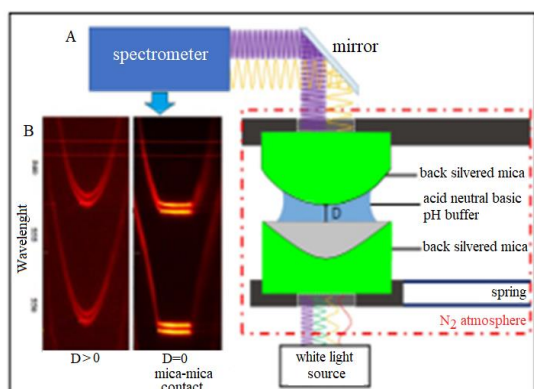


Figure 4: Schematic of the SFA set-up: crossed cylinder experimental set-up of the SFA-MK III (A); resulting fringe pattern of fringes of equal chromatic order, FECO (B). Pvf-5 was adsorbed on both mica surfaces at pH 3 for 20 minutes followed by rinsing with protein-free buffers of variable pH to study the effect of pH on cohesive interaction between Pvf-5 molecules.

All the SFA experiments were carried out using mica as the base surface. Since the freshly cleaved thin sheets of mica are atomically smooth, optically transparent, and chemically inert, they act as ideal substrates for SFA experiments to study adhesive properties of Pvf-5 proteins. The outer opposing sides of mica sheets were coated with a semitransparent layer of silver ( $\sim 55$  nm) using thermal evaporation or chemical sputtering technique. Identically thick and flat back-silvered mica sheets (thickness  $\sim 1$ -5  $\mu\text{m}$ ) were glued with the silver coated side on the cylindrical glass disks (radius of curvature,  $R=1.8$ -2.2 cm) using thermosetting glue (EPON 1007 by Shell). Two semi-transparent curved disks were then mounted orthogonally to each other in an inert nitrogen atmosphere inside an airtight SFA chamber. The top disk was fixed, and the bottom disk was attached to the free end of the double cantilever spring where the stiffness ' $k$ ' of the spring was in the range of 250-950 N/m. The spring and displacement mechanism allowed the motion of opposing disks into a well-defined single asperity contact at a given force.

During the experiment, collimated white light is guided through these disks which act as semi-transparent mirrors. When the surfaces are moved close together, together with the intervening medium it forms a symmetrical three-layer Fabry-Perot interferometer employing MBI. The constructive and destructive interference of the white light at discrete wavelengths leads to the generation of the FECO, which are an infinite series of alternating sharp bright and dark bands which are then detected by the spectrophotometer.

A typical FECO is shown in figure 4 (B), which clearly depicts the flat section of FECO, indicating an extended flat zone of contact. The FECO allows the determination of the inter-mirror distance with a resolution below 1 Å. During the initial contact mica-mica contact in dry nitrogen before adsorbing proteins, the distance  $D=0$  was defined by recording the set of wavelengths. A change in FECO fringe position was used to calculate the shift in distance ( $\Delta D$ ), of two opposing mirrors, where discrete spectral wavelengths of mercury were used to calibrate the spectrograph.

The SFA experiments were performed by precisely approaching the surfaces until they come in adhesive contact followed by retracting them from one another. The adhesive forces were then calculated by using Hooke's law ( $F=k \times \Delta D$ ) where  $k$  is the known stiffness of the spring on which lower surface was mounted and  $\Delta D$  is the shift in distance from the contact (of adhesive surfaces) to their point of separation. Because of the curved geometry of the surfaces, the measured force was normalized by the radius of curvature of the surfaces ( $R$ ). By using the *Derjaguin* approximation, the normalized force  $F(D)/R$  can be directly transformed into the interaction energy per unit area between the two flat surfaces, which is given by  $E(D) = F(D)/2\pi R$ . The error on  $F/R$  was smaller than 0.1 mN/m (force detection threshold) and the error on  $D$  about 0.5 nm.

### 2.3 Sample Preparation for SFA Force Measurements

Mussel adhesive proteins like Pvf-5 are polyelectrolytes possessing ionization tendencies which define their interactions. Therefore, careful selection of pH was made during Pvf-5 adsorption and for buffer solutions used for rinsing the adsorbed proteins (Yu *et al.* 2011a; Danner *et al.* 2012). Also, well defined salt concentration was used to provide sufficient counterions to prevent the electrostatic self-interaction from dominating in the SFA experiments (Lin *et al.* 2007; Yu *et al.* 2011a; Danner *et al.* 2012; Lu *et al.* 2013). Following mica-mica contact in dry air, Pvf-5 proteins were adsorbed on both mica surfaces from 0.02 mg/ml solution of protein in acid saline buffer containing 10 mM acetic acid (AcOH) and 0.25M potassium nitrate ( $\text{KNO}_3$ ) in purified water (Milli-Q grade from Millipore) at pH 3. After a 20 min adsorption, the surfaces were rinsed with protein-free acidic buffer solution.

Following positioning into the SFA, the surfaces were brought almost into contact with a droplet of buffer solution providing a bridge between the two surfaces. To keep the buffer droplet from evaporating, a second droplet of buffer was placed in the box to maintain the vapor pressure.

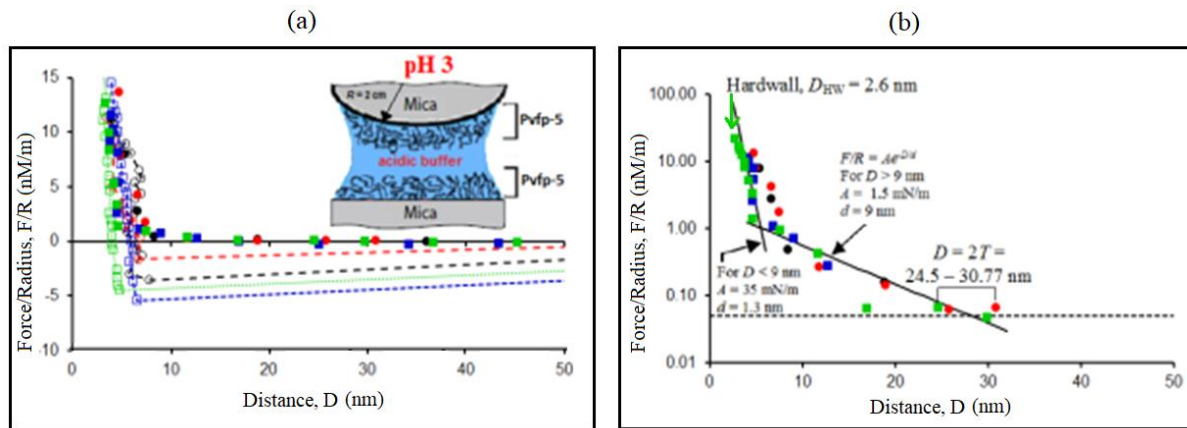


Figure 5: Representative force-distance ( $F-D$ ) profile. (a) Normalized force  $F/R$  measured between two Pvfp-5 coated mica surfaces at pH 3. Positive forces are repulsive and negative forces are attractive. (b) Semi-logarithmic plot showing the range of repulsion  $2T$ , force detection threshold (dotted line) and exponential curves  $F/R=Ae^{-D/d}$ . Solid symbols ( $\bullet$ ,  $\color{red}\bullet$ ,  $\color{blue}\bullet$  and  $\color{green}\bullet$ ) indicate forces on approach and open symbols ( $\circ$ ,  $\color{red}\circ$ ,  $\color{blue}\circ$  and  $\color{green}\circ$ ) indicate forces on retraction of surfaces. Each symbol (circle and square) corresponds to different contact position and different colors indicate different surface approach/retraction cycles.

The influence of pH was investigated by flushing the droplet of acidic buffer ( $\sim 100 \mu\text{L}$ ) with an excess of the new treatment buffer (3ml) with neutral and basic pH. Treatment buffers were

- 1) Neutral saline buffer, 0.25M  $\text{KNO}_3$ , pH  $\approx 7$  (without HCl or NaOH)
- 2) Alkaline/basic saline buffer, 0.25M  $\text{KNO}_3$ , pH  $\approx 10$  (with NaOH)

$\text{KNO}_3$  was used to replace sodium chloride in the buffer solution to avoid corrosion of the thin silver layers under the mica substrates.

Having high concentrations of chloride ions in solution, affect the quality of the optical fringes during the SFA experiments.

Degassed buffer solutions were used for dissolving Pvfp-5 as well as for rinsing. Degassing helps removal of dissolved gases in solution and minimizes the occurrence of bubbles between two surfaces while performing SFA experiments.

Multiple force runs were recorded for each pair of mica and protein adsorption and SFA force measurements were done at a fixed temperature of  $25 \pm 1 \text{ }^\circ\text{C}$ .

## 2 Results and Discussion

Pvfp-5 is the first protein to be secreted by Asian green mussels (*Perna viridis*) in the precisely time regulated secretion of a series of adhesive proteins. Thus, Pvfp-5 is the first protein to initiate contact with the substrate which acts as an adhesive primer. Pvfp-5 is enriched with cysteine and tyrosine (Tyr)/ DOPA residues and its localization at plaque-substrate

interface have provoked interest in its adhesive properties.

Using SFA, the effects of changing pH on adhesion capability of Pvfp-5 was explored. Since Pvfp-5 was adsorbed onto both the opposing mica surfaces, the adhesion forces reported below are proportional to the cohesive interaction between Pvfp-5 molecules.

### 3.1 Adhesion between Pvfp-5 Layers at Acidic pH

Interaction forces ( $F/R$ ) between the thin layers of Pvfp-5 adsorbed symmetrically to both the mica surfaces at acidic pH were measured as a function of separation distance ( $D$ ) (figure 5A). Seven distinct force runs were performed at three different contact positions where the surfaces were brought into contact in the acid saline buffer and then separated after a brief contact time. At pH 3 and 0.25M ionic strength, the maximum adhesion force after separation was measured to be  $F_a/R = 5.42 \text{ mN/m}$ , which can be converted to adhesion energy,  $E = (2/3\pi) F_a/R \approx 1.14 \text{ mJ/m}^2$ . Different force runs displayed variability in adhesion force since factors like contact time or maximum load applied during compression were not explicitly controlled.

However, a clear trend emerged that adhesion decreased with time as the surfaces were repeatedly approached and retracted at the same contact position and as different contact positions were tested. This was most likely due to oxidation of DOPA (Ahn *et al.* 2014; Nicklisch *et al.* 2012). The average value of the adhesion force was  $F/R = 3.63 \text{ mN/m}$ . The repulsive force was recorded for all the force runs during surface approach, showing that adhesion was generated by the formation of adhesive bonds between interacting Pvfp-5 molecules. The force consistently exceeded the

detection threshold of 0.1 mN/m when the surface separation distance  $D$  became smaller than  $2T = 24.5\text{--}30.8$  nm (figure 5B), where  $T$  was the thickness of adsorbed protein layer on one surface. Since the Debye length of the saline buffer was smaller than 1 nm, the recorded long repulsion range ( $2T$ ) can be attributed to the overlap between protein layers adsorbed on opposite surfaces, each having an approximate thickness  $T = 12.2\text{--}15.4$  nm.

The value of the thickness of adsorbed protein layer on mica was larger than the size of Pvfp-5 molecule determined by DLS (Petroni et al. 2015), indicating aggregation behavior of Pvfp-5 molecules at pH 3. The aggregation of Pvfp-5 molecules in solution was also confirmed by dynamic light scattering (DLS) results indicating the hydrodynamic diameter of Pvfp-5 to be 8.56 nm at pH 4, which was most likely via DOPA–DOPA crosslinks.

The maximum value thickness ( $T$ ) of a Pvfp-5 layer on mica substrate was obtained during the first approach, indicating that Pvfp-5 was adsorbed as a soft hydrated layer, as opposed to a compact “hard-wall” coating, allowing the protein molecules and water to rearrange and move as the compressive force was increased. This also indicates that the protein layers were flattened, perhaps due to the formation of additional DOPA-DOPA crosslinks or DOPA-mica hydrogen bonds on compression. Besides, the determination of thickness ( $T$ ) of the adsorbed protein layer on mica substrates, a “hard wall” distance ( $D_{HW}$ ) was also measured using SFA.

Hard wall distance is defined as the asymptotic thickness of confined Pvfp-5 under increasing normal load or pressure. Hard wall distance was determined by compressing the adsorbed Pvfp-5 layer until FECO fringes cease to move towards the lower wavelength side of the signal. The measured hard wall distance for Pvfp-5 at pH 3 was reported to be  $D_{HW} \approx 2.6$  nm.

### 3.2 Adhesion between Pvfp-5 Layers at Neutral pH

Interaction forces ( $F/R$ ) between the thin layers of Pvfp-5 at neutral pH were measured by first adsorbing Pvfp-5 to both mica surfaces at acidic pH, followed by rinsing the surfaces with a protein-free neutral saline solution. At pH 7 and 0.25M ionic strength, the surfaces were brought together and the maximum adhesion force measured after separation was  $F_a/R = 1.28$  mN/m (figure 6A), corresponding to the work of adhesion,  $E = (2/3\pi) F_a/R \approx 0.27$  mJ/m<sup>2</sup>. Maximum adhesion was measured during separation of the first approach-retraction cycle which consequently reduced for the next three force runs recorded on the same contact position.

This trend at pH 7 was similar to that observed at pH 3 earlier, which was most likely due to DOPA

oxidation. The average value of the adhesion force at pH 7 was  $F/R = 0.84$  mN/m. Hysteresis was present for all the force runs recorded and repulsive forces were observed during surface approach with the onset of repulsion at  $2T = 36\text{--}45.8$  nm (figure 6B). Thin hard-wall distance,  $D_{HW} \approx 2.2$  nm was measured at neutral pH.

### 3.3 Adhesion between Pvfp-5 Layers at Basic pH

To assess the interaction forces ( $F/R$ ) between Pvfp-5 layers at basic pH, thin layers of Pvfp-5 were initially adsorbed on both mica surfaces at acidic pH, followed by rinsing with protein-free alkaline buffer solution. Two force runs were recorded at pH 10 and 0.25M ionic strength and small adhesion were measured for both the force runs. The maximum adhesion force measured at pH 10 was 0.68 mN/m (figure 7A), corresponding to a work of adhesion,  $E = 0.14$  mJ/m<sup>2</sup>.

The average value of the adhesion force at pH 10 was  $F/R = 0.6$  mN/m. The approaching branch of force curves revealed a repulsion setting in at a comparably smaller surface separation of  $2T = 11.4\text{--}29.4$  nm than that recorded for acidic and neutral pH (figure 7B). The measured hard wall distance for Pvfp-5 at pH 10 was reported to be  $D_{HW} \approx 3.85$  nm.

### 3.4 Discussion

*Mytilus edulis* foot protein-5 (Mefp-5) is one of the adhesive proteins in the byssal adhesive plaque of the mussels of *M. edulis* that has been reported to have highest molecular DOPA concentration which is localized near the plaque substrate interface similar to Pvfp-5 (Danner et al. 2012, Petroni et al. 2015). The adhesion capabilities of Pvfp-5 were assessed by SFA experiments using mica as the substrate, which enabled direct comparison of Pvfp-5 with extensively studied Mefp-5. Strong adhesion force was consistently measured between symmetrically adsorbed Pvfp-5 films at pH 3 (maximum adhesion force,  $F_a/R = 5.42$  mN/m).

Previous studies on Mefp-5 showed adhesion force,  $F_a/R = 6.0$  mN/m, which slightly exceeded the adhesion force of Pvfp-5. Considering the 30 mol% DOPA content of Mefp-5 compared to 11 mol% DOPA in Pvfp-5, the adhesion force between interacting proteins films of both the adhesive proteins were not significantly different (Danner et al. 2012).

It has been reported that exposure of Mefp-5 to pH above 7.5 reduces its adhesion by 95% due to rapid oxidation of DOPA to Dopaquinone (Kan et al. 2014). However, the CYS-enriched Pvfp-5 was adhesive at both neutral and basic pH with the maximum adhesion force,  $F_a/R = 1.28$  mN/m at pH 7.0 and  $F_a/R = 0.68$  mN/m at pH 10 (table 1).

Thus, increasing the pH of gap solution from pH3 to pH7 and pH10, reduced the adhesion force by approximately 75% and 87%, respectively, compared to initial adhesion force measured at acidic pH. Therefore, CYS residues in the amino acid sequence of Pvfp-5 participate in the reduction of quinones by providing a pH-dependent antioxidant activity to Pvfp-5, the first protein secreted by *P. viridis*, justifying its role as a vanguard protein that acts as an

adhesive primer which initiates first adhesive interactions with the substrate.

Besides adhesion, table 1 summarizes the variation of other parameters with respect to change in pH conditions which reveals an important trend: the hard wall and the thickness ( $T$ ) of Pvfp-5 layer on mica, changed with pH.

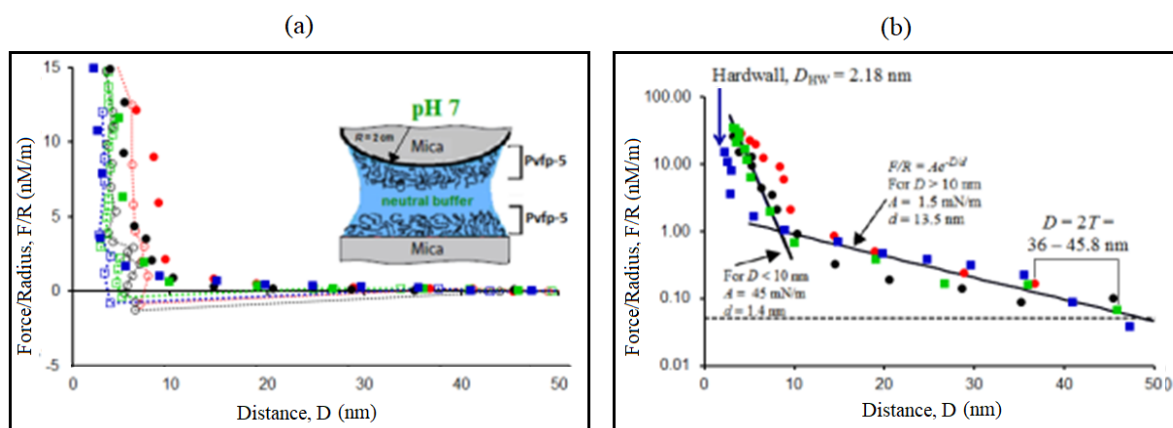


Figure 6: Representative force-distance ( $F-D$ ) profile. (a) Normalized force  $F/R$  measured between two Pvfp-5 coated mica surfaces at neutral pH ( $=7$ ). (b) Semi-logarithmic plot showing the range of repulsion  $2T$ , force detection threshold (dotted line) and exponential curves  $F/R=Ae^{-D/d}$ . Solid symbols ( $\bullet$ ,  $\bullet$ ,  $\blacksquare$  and  $\blacksquare$ ) indicate forces on approach and open symbols ( $\circ$ ,  $\circ$ ,  $\square$  and  $\square$ ) indicate forces on retraction of surfaces. Each symbol (circle and square) corresponds to different contact position and different colors indicate different surface approach/retraction cycles.

Table 1: Summary of various parameters for Pvfp-5 interactions in symmetric configuration measured by SFA.

pH	Max. adhesion force, $F_a/R$ (mN/m)	Max. adhesion energy, $E$ (mJ/m <sup>2</sup> )	Pvfp-5 film thickness, $T$ (nm)	Hardwall distance, $D_{HW}$ (nm)
pH 3	5.42	1.14	12.2 – 15.4	2.6
pH 7	1.28	0.27	18 – 22.9	2.2
pH 10	0.68	0.14	5.7 – 14.7	3.8

The film thickness ( $T$ ) of Pvfp-5 on mica at pH 3 was in the range 12.2-15.4 nm with hard wall,  $D_{HW}$  (pH 3)  $\approx$  2.6 nm. After increasing the pH of the gap solution to 7.0, repulsion at comparatively higher distance was noticed during approach.

The film thickness ( $T$ ) at pH 7 was measured to in the range of 18-22.9 nm with hard wall,  $D_{HW}$  (pH 7)  $\approx$  2.2 nm.

The increase in film thickness at pH 7 suggests that the Pvfp-5 film expands at neutral pH; however, the hard wall distance measured on compression remained almost unchanged.

When the pH of the gap solution was changed from acidic to alkaline, significantly low repulsion range corresponding to film thickness ( $T$ ) in the range 5.7-14.7 nm was recorded. Surprisingly, the hard wall distance measured upon compressing the Pvfp-5 layer under higher loads was  $D_{HW}$  (pH 10) = 3.8 nm, which was higher than  $D_{HW}$  recorded at pH 3 and pH 7, respectively.

Lower film thickness and higher hard wall at pH 10 suggests a more compact and rigid conformation of Pvfp-5, which may prevent the exposure of DOPA residues to higher pH, thus preventing DOPA from spontaneous oxidation.

Surprisingly, SFA experiments on Pvfp-5 also showed that adsorption of thicker layers of protein on mica resulted in diminished adhesion (results not shown).

Series of experiments performed with varying adsorption time and protein concentration in solution revealed that thinner layer have more exposed DOPA

molecules available to interact and form adhesive bonds whereas, thicker layers screen DOPA molecules as well as enhances cross-linking between DOPA molecules making them unavailable for subsequent adhesive interactions.

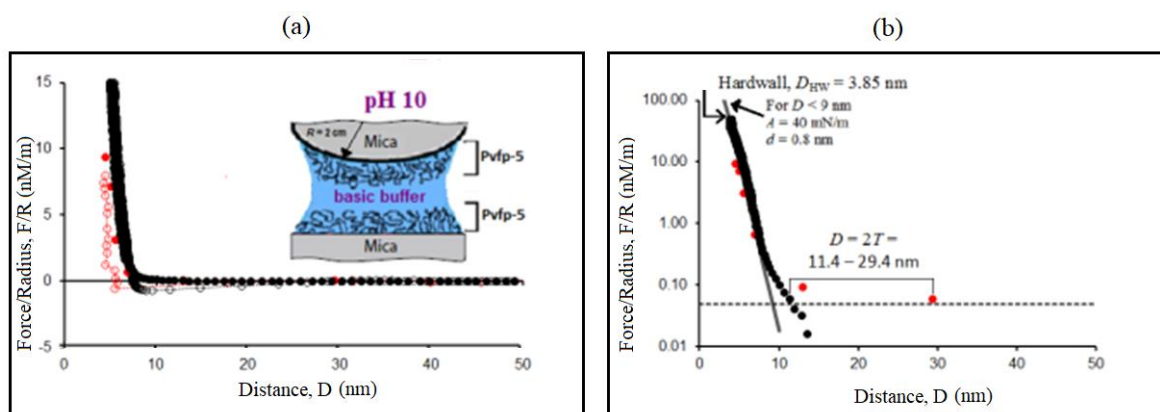


Figure 7: Representative force-distance ( $F-D$ ) profile: (A) Normalized force  $F/R$  measured between two Pvfp-5 coated mica surfaces at pH 10. (B) Semi-logarithmic plot showing the range of repulsion  $2T$ , force detection threshold (dotted line) and exponential curves  $F/R=Ae^{-D/d}$ . Solid symbols (● and ●) indicate forces on approach and open symbols (○ and ○) indicate forces on retraction of surfaces. Different colors indicate different surface approach/retraction cycles.

## 4 Conclusion

In summary, the objective of this work was understanding the molecular interactions between Pvfp-5 proteins adsorbed on mica substrates at different pH conditions using the SFA technique. The results provide important insights into the wet adhesion mechanism of Asian green mussels (*P. Viridis*), whereby a DOPA-rich primer (Pvfp-5) is initially secreted because of its superior adsorptive and adhesive abilities to interact with foreign surfaces.

Other experimental studies of Pvfp-5 shows the ability of Pvfp-5 to act as an adhesive primer to displace surface-bound water from hydrophilic surfaces allows the formation of strong and durable bonds via its adhesive DOPA residues exposed on the protein surface, hence creating an environment conducive to the assembly of other plaque components (Petroni *et al.* 2015).

By studying the effects of changing pH on adhesive properties of Pvfp-5, the emerging picture is that Pvfp-5 with its high DOPA and CYS-content, maintains adhesion even at higher pH and acts as a self-antioxidant, overcoming the spontaneous oxidation of DOPA to quinone at higher seawater pH (~ 8) with saturating levels of dissolved oxygen. Also, tyrosine, DOPA and cysteine motifs in Pvfp-5 play a key role

in enabling the robust underwater adhesion exhibited by *P. viridis*.

More broadly, the study provided a molecular basis for understanding the impressive underwater adhesion of marine organisms, an insight that should prove relevant for diverse areas, from designing of mussel inspired bioadhesives to engineering targeted anti-fouling strategies.

DOPA- and CYS- containing proteins like Pvfp-5 are crucial for wet adhesion in mussels that retards oxidation by shielding the amino acids from the solvent and endowing the protein with the ability to maintain adhesion at neutral as well as basic pH levels (Kaushik *et al.* 2015). Recent studies on the underwater adhesion mechanisms of marine fouling organisms have been explored by SFA, where three key mechanisms of successful underwater adhesion, i.e. DOPA and REDOX chemistry, cation- $\pi$  interactions and complex coacervation, have been suggested (Hwang *et al.* 2010; Yu *et al.* 2011; Gebbie *et al.* 2017).

SFA and other techniques have not yet fully elucidated all the adhesion mechanisms of the marine fouling organisms like mussels, but the key mechanisms exploited should be effective strategies for the development of bio-inspired medical adhesives and tissue sealants, antifouling surfaces for medical devices and environmentally friendly antifouling



paints for use in the marine industry. Further, understanding the aspects of natural redox control can provide fundamentally important insights for adhesive polymer engineering, surface modifications and antifouling strategies.

## Interest Conflict

The authors declare that they have no conflict of interest.

## Acknowledgment

We would like to thank Prof. Ali Miserez (NTU, Singapore) for providing the isolated and purified mussel foot proteins. This research was supported by the University of Calabria (Unical), Italy through its doctoral fellowship to N. J. Patil under Bernardino Telesio School of Science and Technique. We thank CNR-Nanotec and Department of Physics, Unical for various experimental and computing facilities.

## References

Comyn, J. (1981). *The relationship between joint durability and water diffusion. In Developments in Adhesives*; Kinloch, A. J., Edition, U.K.: Applied Science Publishers: Barking, Vol. 2, 279-313.

Danner, E. W., Kan, Y., Hammer, M. U., Israelachvili, J. & Waite, H. (2012). Adhesion of Mussel Foot Protein Mefp-5 to Mica: An Underwater Superglue. *Biochem*, 51(33), 6511–6518.

DeMartini, D. G., Errico, J. M., Sjoestroem, S., Fenster, A. & Waite, H. J. (2017). A cohort of new adhesive proteins identified from transcriptomic analysis of mussel foot glands. *J R Soc Interface*, 14(131), 0151.

Ditsche, P. & Summers, A. P. (2014). Aquatic versus terrestrial attachment: Water makes a difference. *Beilstein J Nanotechnol*, 5, 2424–2439.

Gebbie, M. A., Wei, W., Schrader, A. M., Cristiani, T. R., Dobbs, H. A., Idso, M., Chmelka, B. F., Waite, H. & Israelachvili, J. N. (2017). Tuning underwater adhesion with cation- $\pi$  interactions. *Nat Chem*, 9, 473-479.

Hamada, N. A., Roman, V. A., Howell, S. M. & Wilker, J. J. (2017). Examining Potential Active Tempering of Adhesive Curing by Marine Mussels. *Biomim*, 2(16), doi: 10.3390/biomimetics2030016.

Hwang, D. S., Zeng, H., Masic, A., Harrington, M. J., Israelachvili, J. N. & Waite, J. H. (2010). Protein- and metal-dependent interactions of a prominent protein in mussel adhesive plaques. *J Biol Chem*, 285(33), 25850–25858.

Hwang, D. S., Zeng, H., Srivastava, A., Krogstad, D. V., Tirrell, M., Israelachvili, J. N. & Waite, H. J. (2010). *Viscosity and interfacial properties in a mussel-inspired adhesive coacervate. Soft Matter*, 6, 3232–3236.

Israelachvili, J. N. & McGuiggan, P. M. (1990). Adhesion and short-range forces between surfaces. Part I: new apparatus for surface force measurements. *J Mater Res*, 5, 2223–2231.

Kan, Y., Danner, E. W., Israelachvili, J. N. & Waite, H. (2014). Boronate Complex Formation with Dopa Containing Mussel Adhesive Protein Retards pH-Induced Oxidation and Enables Adhesion to Mica. *PLoS ONE*, 9(10), doi: 10.1371/journal.pone.0108869.

Kaushik, N. K., Kaushik, N., Pardeshi, S., Sharma, J. G., Lee, S. H. & Choi, E. H. (2015). Biomedical and Clinical Importance of Mussel-Inspired Polymers and Materials. *Mar Drugs*, 13, 6792-6817.

Kollbe Ahn, B. (2017). Perspectives on Mussel-Inspired Wet Adhesion. *J Am Chem Soc*, 139, 10166–10171.

Lee, H. S., Scherer, N. F. & Messersmith, P. B. (2006). Single-molecule mechanics of mussel adhesion. *Proc Natl Acad Sci U S A*, 103, 12999–13003.

Lee, B. P., Messersmith, P. B., Israelachvili, J. N. & Waite, J. H. (2011). Mussel-Inspired Adhesives and Coatings. *Annu Rev Mater Res*, 41, 99–132.

Lin, Q., Gourdon, D., Sun, C., Holten-Andersen, N., Anderson, T. H., Waite, J. H. & Israelachvili, J. N. (2007). Adhesion mechanisms of the mussel foot proteins mfp-1 and mfp-3. *Proc Natl Acad Sci U S A*, 104(10), 3782-3786.

Lu, Q., Danner, E., Waite, J. H., Israelachvili, J. N., Zeng, H. & Hwang, D. S. (2013). Adhesion of mussel foot proteins to different substrate surfaces. *J Roy Soc Interf*, 10(79), 1–11.

Menyo, M. S., Hawker, C. J. & Waite, J. H. (2013). Versatile tuning of supramolecular hydrogels through metal complexation of oxidation-resistant catechol-inspired ligands. *Soft Matter*, 9(43), 10314-10323.

Ornes, S. (2013). Mussels' sticky feet lead to applications. *Proc Natl Acad Sci U S A*, 110(42), 16697-9.

Petrone, P., Kumar, A., Sutanto, C. N., Patil, N. J., Kannan, S., Palaniappan, A., Amini, S., Zappone, B., Verma, C. & Miserez, A. (2015). Mussel adhesion is dictated by time-regulated secretion and molecular conformation of mussel adhesive proteins. *Nat comm*, 6, 8737.

Priemel, T., Degtyar, E., Dean, M. N. & Harrington, M. J. (2017). Rapid self-assembly of complex biomolecular architectures during mussel byssus biofabrication. *Nat Comm*, 8, 14539.

Silverman, H. G. & Roberto, F. F. (2007). Understanding marine mussel adhesion. *Mar Biotech*, 9(6), 661–681.

Stewart, R. J., Ransom, T. C. & Hlady, V. (2011). Natural Underwater Adhesives. *J Polym Sci B Polym Phys*, 49(11), 757-771.

Waite, J. H., Andersen, N. H., Jewhurst, S. & Sun, C. J. (2005). Mussel Adhesion: Finding the Tricks Worth Mimicking. *J Adhes*, 81, 297–317.

- Wei, W., Yu, J., Broomell, C., Israelachvili, J. N. & Waite, J. H. (2013). Hydrophobic enhancement of Dopa-mediated adhesion in a mussel foot protein. *J Am Chem Soc*, 135, 377–383.
- Wilker, J. J. (2010). Marine bioinorganic materials: mussels pumping iron. *Curr Opin Chem Biol*, 14, 276–283.
- Wilker, J.J. (2015). BIOLOGICAL ADHESIVES. Positive charges and underwater adhesion. *Science*, 349(6248), 582-3.
- Yu, J., Kan, Y., Rapp, M., Danner, E., Das, S., Miller, D. R., Chen, Y., Waite, J. H & Israelachvili, J. N. (2013). Adaptive hydrophobic and hydrophilic interactions of mussel foot proteins with organic thin films. *Proc Natl Acad Sci U S A*, 110, 15680–15685.
- Yu, J., Wei, W., Danner, E., Ashley, R. K., Israelachvili, J. N. & Waite, J. H. (2011a). Mussel protein adhesion depends on thiol-mediated redox modulation. *Nat Chem Biol*, 7, 588–590.
- Yu, J., Wei, W., Danner, E., Israelachvili, J. N. & Waite, H. J. (2011b). Effects of Interfacial Redox in Mussel Adhesive Protein Films on Mica. *Adv Mater*, 23(20), 2362–2366. doi:10.1002/adma.201003580.